A novel approach to multispectral blind image fusion

Deepa Kundur[a], Dimitrios Hatzinakos[a] and Henry Leung[b]

[a]Department of Electrical and Computer Engineering
University of Toronto
Toronto, Ontario Canada M5S 3G4

[b]Department of National Defense
Defense Research Establishment Ottawa
Building 29, 3701 Carling Avenue
Ottawa, Ontario Canada K1A 0Z4

ABSTRACT

In this paper we propose a robust method of data fusion for the classification of multispectral images. The approach is novel in that it attempts to remove blurring of the images in conjunction with fusing the data. This produces a more robust and accurate overall classification scheme. The approach is applicable to situations in which registered multispectral images of the same scene are available.

The novel scheme is comprised of three main stages. The first stage involves the blind restoration of the degraded multispectral images to combat blurring effects. The results are fused in the second stage with a statistical classification method which performs both pixel-level and intermediate-level classification. The classification output is then passed through a final stage which provides a relative measure of the success of the classification method. This information is fed back to the first stage to improve the reliability of the restoration method. The performance of the proposed scheme is demonstrated by applying the technique to simulated and real photographic data. The simulation results demonstrate the potential of the method for robust classification of degraded data.

Keywords: sensor fusion, multispectral classification, blind image restoration

1. INTRODUCTION

The inaccuracy of many image sensor fusion strategies often results from attempting to fuse data that exhibits motion-induced blurring or "defocussing" effects. Compensation for such blurring is inherently sensor-dependent and is not trivial as the exact blur is often time-varying and unknown.[1] In such a situation, restoration is frequently performed on the degraded data prior to fusion. The two main obstacles with performing image restoration are: 1) the blurring function may not be explicitly known and it may be infeasible to measure it, 2) the image restoration problem is inherently ill-posed due to the presence of additive noise on the degraded image or because the blurring function is bandlimited which results in a loss of the image information content.

The first obstacle may be overcome by using blind image restoration algorithms. *Blind image restoration* refers to the dual process of blur identification and image restoration and is used in situations where only partial information about the image degradation process is available. Blind image restoration is suited for situations in which the blurring and noise characteristics of the imaging system may be unknown due to their time-varying nature. A recent survey of such algorithms can be found in Ref. 2.

The weakness of most techniques stems from their numerical instability; there is often insufficient information to provide an accurate regularized solution to the problem and noise amplification may result.[3] In addition, it may be impractical for a human observer to supervise the restorations to prevent instability. This may result in an unreliable image estimate, which in turn can effect the accuracy of subsequent higher-level processing of the images. Thus,

Contact author information: (Send correspondence to D.H.)
D.H.: Email: dimitris@comm.toronto.edu; Telephone: 416-978-1613; Fax: 416-978-4425; This work was supported by the Canadian Department of National Defense under Contract 08SV.W7714-6-9990.

fusion of a degraded image with other image data can be compromised due to the ill-posed nature of the restoration process.

In this paper we present a novel approach which performs the dual task of image restoration and fusion for the classification of multispectral imagery. The method is comprised of three stages. In the first stage, the degraded images are passed through a blind image restoration algorithm. The output of this stage is passed through a classification algorithm which fuses the images. The classified output is evaluated in a final stage to obtain a rough estimate of the reliability of the restoration. This information is fed back to aid the image restoration process. We refer to the approach as *blind image fusion.*

In the next section we introduce the novel blind image fusion method; we discuss an application of the approach for classification in Section 3. In Section 4, we present simulation results on synthetic and real data to show its potential for robust blind classification of multispectral imagery. Concluding remarks are provided in Section 5.

2. PROPOSED METHOD

2.1. General approach

In this section we provide general overview of the proposed technique. The main objective of the proposed blind fusion scheme is to perform improved image fusion in the presence of unknown image degradation. The task of image restoration is often performed prior to and separate from fusion. This solution is suboptimal as the information from the fusion process can often contain relevant information to improve the restoration which can in turn provide improved fusion.

We call the proposed method *blind* because it does not require knowledge of the blurring process during image acquisition. Since the objective of the procedure is to fuse several multispectral images of the same scene, we call our novel method a *blind image fusion* technique. The authors are unaware of the existence of other blind fusion methods for classification.

In the proposed method we make use of the smoothness properties of the original image to provide an estimate of the accuracy of the blind image restoration stage. The numerical instability of a restoration method often manifests itself as excessive noise amplification on the restored result.[3] Thus, a measure of smoothness of the restoration can be used to indicate possible inaccuracy of the result. Often the visual quality of the restored image is not a good indicator of the reliability of higher level processing tasks such as fusion. For example, for classification the visual quality of an image is not the best indicator for classification accuracy. In fact a restoration that provides a good classification may not be visually similar to the original unblurred image. Therefore, to improve the reliability of the fusion process, it is important to make use of information from the higher level processing stage to enhance the restoration stage. Figure 1 gives a summary of the proposed approach.

A selection of algorithms can be used in each stage of the approach. We provide one possible algorithmic implementation of the method, in Section 3. to demonstrate the potential of the approach for blind fusion. We give reasons for using the specific algorithms.

In the next two sections we discuss the task of blind image restoration and discuss the process of image fusion for classification.

2.2. Blind deconvolution for image restoration

In this paper we assume that the acquired image follows the common linear degradation model given by,[3]

$$g(m,n) = h(m,n) * f(m,n) + w(m,n) \tag{1}$$

where (m,n) represents the discrete pixel coordinates, $f(m,n)$ is the true image, $h(m,n)$ is the blur (also known as the point spread function (PSF)), and $w(m,n)$ is the additive noise in the system. In this simplified model the observed image $g(m,n)$, true image $f(m,n)$ and noise $w(m,n)$ are coupled linearly, so the problem of recovering $f(m,n)$ from $g(m,n)$ is referred to as the *linear image restoration problem.*[4] If we neglect the presence of additive noise, then we may approximate the degradation model by,

$$g(m,n) = h(m,n) * f(m,n). \tag{2}$$

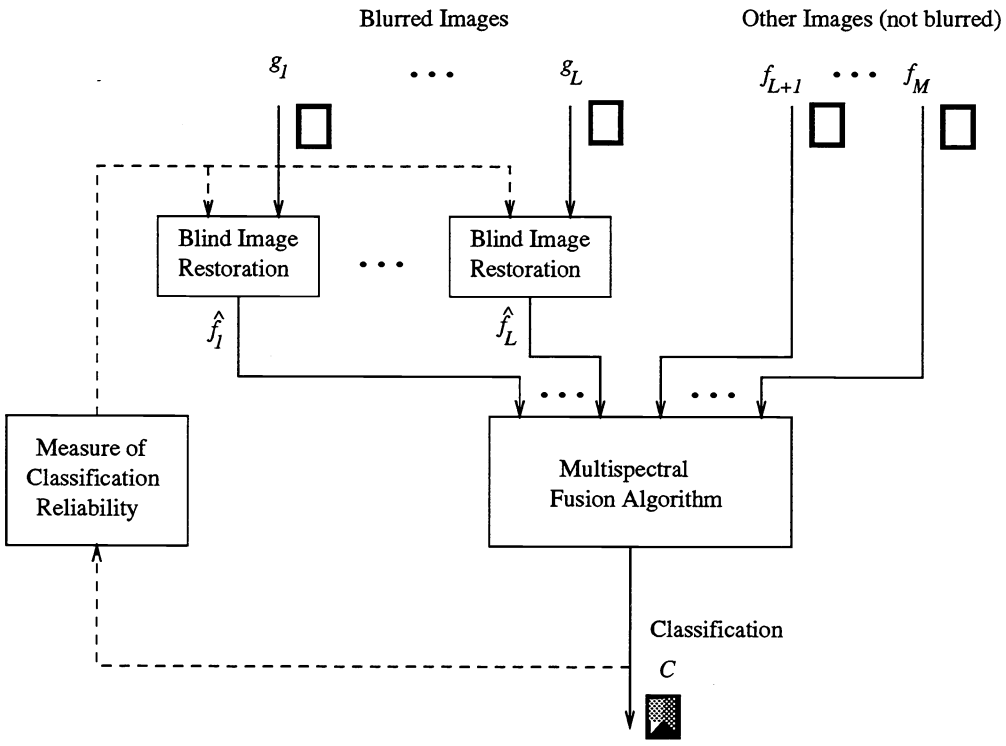

Figure 1. Proposed Multichannel Blind Image Fusion Approach.

The process of recovering $f(m,n)$ from $g(m,n)$ becomes that of *deconvolving* $h(m,n)$ from $g(m,n)$.

In applications such as remote sensing where the blur characteristics are often time-varying the explicit form of the degradation is not known. The restoration task involves the process of simultaneously estimating the PSF (or its inverse) and restoring true image using partial information about the imaging system; this is known as blind image restoration. For situations in which the degradation process can be represented by Equation (2), the restoration procedure is known as *blind image deconvolution.*[2]

A number of blind image deconvolution techniques have been recently proposed.[2] Most methods suffer from a poor compromise between reliability, computational complexity and portability. Another limitation of many methods is their sensitivity to additive noise in the degraded image. Since most blurs are low pass, deconvolution requires high pass filtering the image to undo the blur. As a result the high frequency components of the additive noise become amplified resulting in numerical instability of the restoration process. Thus, the blind image deconvolution problem is ill-posed. Smoothness information about the true image can be used to regularize the problem.

In this paper we implement an iterative blind deconvolution method for image restoration. It has been shown that iterative restoration methods exhibit noise amplification as the iterations progress.[5] A successful method to prevent noise amplification is to terminate the restoration process before numerical instability results. The novel approach we present makes use of information from the fusion stage to find an optimal point to terminate the restoration procedure.

2.3. Multichannel image classification

In this paper we assume that the ultimate goal of the image fusion process is to produce an accurate scene classification. Classification is an information processing task in which specific entities are mapped to general categories. For the application of classification to multichannel or multispectral imagery, the specific goal is to assign each vector-valued pixel of the multispectral image to its appropriate classification category using tonal or textural data.[6] Many

techniques for classification exist (see Refs. 6, 7, 8, 9, 10, 11 and references therein). In this paper we consider the fusion of multichannel imagery by classification using tonal information from the different frequency channels.

A measure of restoration reliability is obtained from the classification results and is fed back to aid the restoration stage. This specific measure is discussed in Section 3.4. In the next section we discuss the specific algorithmic details for implementation of the proposed multispectral blind fusion approach.

3. IMPLEMENTATION OF THE BLIND FUSION ALGORITHM

For the implementation of the proposed blind fusion method shown in Figure 1 we make use of two successful algorithms: the Nonnegativity and Support constraints Recursive Inverse Filtering (NAS-RIF) algorithm[12] and the MRF multispectral classification method by Solberg *et. al.*[11] A number of different algorithms can be used at each stage, but we have selected these particular methods as they are well-suited for the problem we are addressing in this paper.

For simplicity we will consider the situation of classifying two images of the same scene: a noisy or low resolution image giving only partial classification information about the scene, and a high resolution blurred image. The goal of the proposed method is to restore the blurred image such that it can be properly fused to produce an accurate classification. We describe the overall implementation in Section 3.4.

3.1. The NAS-RIF algorithm

The Nonnegativity and Support Constraints Recursive Inverse Filtering (NAS-RIF) algorithm[12] is applicable to situations in which an object of finite support is imaged against a uniform background. Figure 2 gives an overview of the algorithm. The blurred image pixels $g(m,n)$ are input to a 2-D variable coefficient FIR filter $u(m,n)$ whose output represents an estimate of the true image denoted $\hat{f}(m,n)$. This estimate is then mapped to the set of all nonnegative images of given finite support by replacing the negative pixels with zero and the pixels outside the region of support with the appropriate background pixel colour value L_B to produce $\hat{f}_{NL}(m,n)$. The difference between $\hat{f}$ and $\hat{f}_{NL}$ is used to update the filter u. The algorithm involves the minimization of the following convex cost function with respect to $u(m,n)$:

$$
\begin{aligned}
J &= \sum_{\forall(m,n)} \left[\hat{f}_{NL}(m,n) - \hat{f}(m,n)\right]^2 \\
&= \sum_{(m,n)\in D_{sup}} \hat{f}^2(m,n) \left[\frac{1-\mathrm{sgn}(\hat{f}(m,n))}{2}\right] + \sum_{(m,n)\in \overline{D}_{sup}} [\hat{f}(m,n) - L_B]^2 + \gamma \left[\sum_{\forall(m,n)} u(m,n) - 1\right]^2
\end{aligned} \tag{3}
$$

where $\hat{f}(m,n) = g(m,n) * u(m,n)$, and $\mathrm{sgn}(f) = -1$ if $f < 0$ and $\mathrm{sgn}(f) = 1$, if $f \geq 0$. D_{sup} is the set of all pixels inside the region of support, and $\overline{D}_{sup}$ is the set of all pixels outside the region of support. The support is defined as the smallest rectangle which can completely encompass the true unblurred object. The variable γ in third term of the equation is nonzero only when L_B is zero, ie., the background colour is black. The third term is used to constrain the parameters away from the trivial all-zero global minimum for this situation.[13] The user-specified parameters in the algorithm are the FIR filter dimensions, the unblurred object support and the parameter γ.

The main advantage of the NAS-RIF method is its superior convergence properties to other techniques of its class.[2] In addition it is based on well-developed theory and is not computationally complex.[13] The major disadvantage is the excessive noise amplification that results due to the ill-posed nature of the blind deconvolution problem. One successful method of combating the numerical instability is to terminate the algorithm before excessive noise occurs in the restored output.[13] In this paper, we use the output of the classification stage to determine a good stopping criterion.

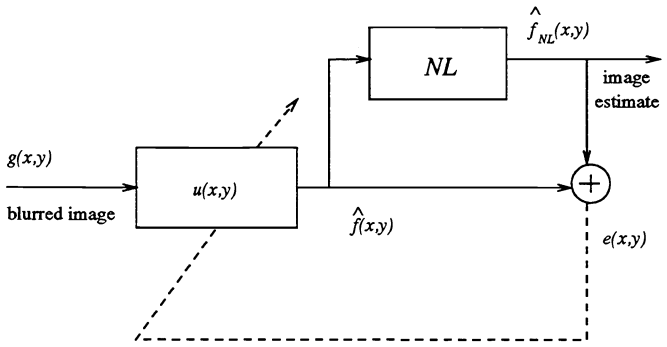

Figure 2. The NAS-RIF Algorithm for Blind Image Deconvolution.

3.2. Statistical classification using MRFs

Markov random field (MRF) models provide a methodological framework which allows the images from the different sensors to be merged statistically in a consistent way. The MRF classification method by Solberg *et. al.*[11] uses the MRF models to form a likelihood function. The goal of the method is to find a classification that maximizes the posterior (MAP) distribution of the likelihood function. Determination of this MAP estimate requires the minimization of a sum of *energy functions*. The prior information used for classification and the observed image data can be easily combined through the use of these energy functions.[11] The flexibility and success of the method in incorporating spatial, spectral and temporal contextual information makes it an attractive method to implement for blind image fusion.

In this paper we assume that the multisource images are taken close in time so that temporal changes in the scene are negligible; we assume no existence of old ground truth maps to aid the classification process. Based on the above constraints, the MAP classification estimate for pixel (m, n) will require the minimization of the following function with respect to the classified image C,[11]

$$U(\hat{f}_1, \hat{f}_2, \ldots, \hat{f}_M, C) = \sum_{s=1}^{M} \alpha_s U_{data}(\hat{f}_s(m,n), C(m,n)) + U_{sp}(C) \tag{4}$$

where the subscript s denotes data from a particular sensor, α_s is the sensor-specific reliability factor (usually taken to be the individual sensor classification accuracy), M is the number of images being fused, U_{data} is the sensor-specific image statistic function, U_{sp} is the spatial context energy function, and $\hat{f}_s$ is the restored image from sensor s. C is the overall classified image and is the same dimension as the input images $\hat{f}_1, \ldots, \hat{f}_M$.

In the simulations performed we assume that the image noise statistics can be modelled by a normal distribution and that the noise processes are independent from one another. U_{data} is given by,[11]

$$U_{data}(\hat{f}_s(m,n), C(m,n)) = \frac{1}{2}\ln|2\pi\sigma_c^2| + \frac{1}{2\sigma_c^2}\left(\hat{f}_s(m,n) - \mu_c\right)^2 \tag{5}$$

where σ_c^2 and μ_c are the class-conditional variance and the mean value for class $C(m,n)$, respectively. The spatial context function is given by,[11]

$$U_{sp}(C) = \beta_{sp} \sum_{(k,l)\in G_{(m,n)}} I(C(m,n), C(k,l)) \tag{6}$$

where $G_{(m,n)}$ is the set of all pixels adjacent and diagonal to (m,n), β_{sp} is a user-specified parameter and $I(\cdot,\cdot)$ is given by

$$I(c_1, c_2) = \begin{cases} -1 & \text{if } c_1 = c_2 \\ 0 & \text{if } c_1 \neq c_2 \end{cases} . \tag{7}$$

Equation (4) is not convex for $\beta_{sp} \neq 0$, so we implement the minimization routine using Besag's iterate conditional modes (ICM) algorithm as suggested in Ref. 11. The algorithm can potentially become trapped in local minima, but this was not a problem during the actual simulations performed.

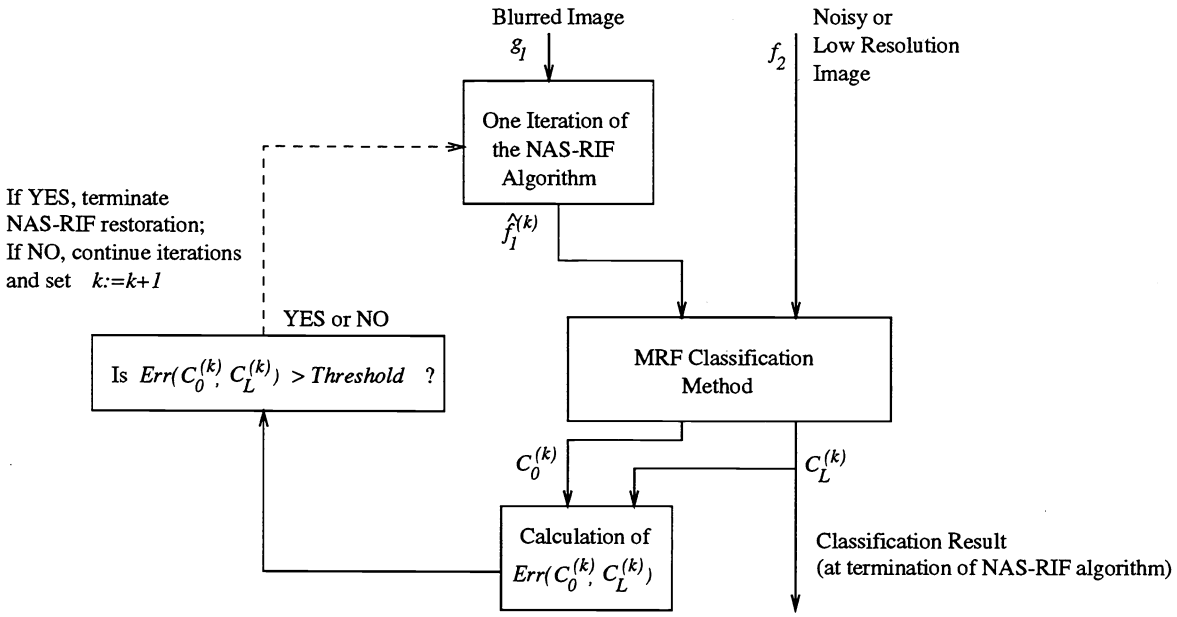

Figure 3. Implementation of the Proposed Blind Image Fusion Method

3.3. Calculation of noise statistics for the restored images

The MRF classification method requires knowledge of the variance of the additive noise. We may estimate the variance of noise for a particular image estimate $\hat{f}$ as follows. At a particular iteration of the NAS-RIF algorithm we can represent the image estimate by

$$\hat{f}(m,n) = g(m,n) * u(m,n) \tag{8}$$

where $u(m,n)$ is the current value of the FIR filter coefficients and $g(m,n)$ is the degraded image. If we assume the linear degradation model of Equation (1) then we may represent $\hat{f}$ as

$$\hat{f}(m,n) = f(m,n) * h(m,n) * u(m,n) + w(m,n) * u(m,n) = \tilde{f}(m,n) + \tilde{w}(m,n) \tag{9}$$

where $\tilde{f} = f * h * u$ is the image estimate at the current iteration and $\tilde{w} = w * u$ is the associated additive noise. If we assume that $\tilde{f}$ is somewhat similar to the ideal image then we may consider $\hat{f}$ to be a noisy version of the true image f with the mean and variance of the noise given by those of $\tilde{w}$. Assuming that w is zero mean with variance σ_w^2, it is easy to show that $\tilde{w}$ is also zero mean with variance $\sigma_{\tilde{w}}^2 = \sigma_w^2 \sum_{\forall(m,n)} u^2(m,n)$. We use this relation to estimate the noise variance in our simulations.

3.4. Stopping criterion

The major limitation of the NAS-RIF algorithm is the difficulty in determining a good termination point for success classification. In this section we propose a good stopping criterion.

Figure 3 gives an overview of the proposed blind fusion scheme. For simplicity we consider the fusion of a blurred image g_1 (which follows the linear degradation model of Equation (1)) and a noisy image of the same scene f_2. Both images are assumed to be registered. At each iteration of the NAS-RIF algorithm, the restoration of g_1 denoted $\hat{f}_1^{(k)}$ (where k is the current iteration) is passed through the classification method discussed in Section 3.2. Classification of $\hat{f}_1^{(k)}$ and f_2 is performed twice using two different β_{sp} values: $\beta_{sp} = 0$ and $\beta_{sp} = \beta_L$, where $\beta_L > 0$. We denote the classification results corresponding to $\beta_{sp} = 0$ and $\beta_{sp} = \beta_L$ by $C_0^{(k)}$ and $C_L^{(k)}$, respectively. A measure of the

difference between $C_0^{(k)}$ and $C_L^{(k)}$ is used to determine the possibility of noise amplification effecting the fusion results. This measure is given by,

$$Err(C_0^{(k)}, C_L^{(k)}) = \frac{\sum_{\forall(m,n)} \tilde{I}(C_0^{(k)}(m,n), C_L^{(k)}(m,n))}{N} \times 100 \tag{10}$$

where N is the number of pixels in C_0 or C_L, and $\tilde{I}(c_0, c_L) = 1$ if $c_0 = c_L$ and $\tilde{I}(c_0, c_L) = 0$ otherwise. If this difference increases dramatically from one iteration to the next, then the algorithm is terminated and the classified output is taken to be $C_L^{(k-1)}$ where k is the current iteration.

As discussed in Section 3.2. the fusion procedure involves the minimization of Equation (4) which is comprised of two terms; a sensor-specific component involving U_{data}, and a spatial context function U_{sp}. The β_{sp} parameter governs the relative importance of U_{sp}. If we consider the case where $\beta_{sp} = 0$, then the classification process is equivalent to pixel-level fusion. When $\beta_{sp} > 0$, the classification is equivalent to an intermediate-level fusion in which the classification of a pixel depends on that of its eight nearest neighbours. The larger the values of β_{sp} the stronger the effect of U_{sp} and the smoother the classification.

Given a restored image $\hat{f} = \tilde{f} + \tilde{w}$, its variance is a result of two sources, the variance of $\tilde{f}$ and the variance of $\tilde{w}$ denoted $\sigma_{\tilde{f}}^2$ and $\sigma_{\tilde{w}}^2$, respectively. For excessive noise amplification the variance of $\tilde{w}$ dominates. Examination of Equations (4), (5) and (6) suggest that for excessive noise amplification $\sigma_{\tilde{w}}^{2*}$ would be large and U_{sp} would have a more pronounced effect on the classification results for $\beta_{sp} > 0$. Similarly, when the noise variance is low relative to the true image, U_{sp} has less effect on the outcome. Therefore, it is reasonable to assume that if noise amplification is significantly effecting the classification, then the relative difference between $C_0^{(k)}$ and $C_L^{(k)}$ at iteration k would be large.

4. SIMULATION RESULTS

4.1. Basis of evaluation

The measure we use to evaluate the success of the classification task is the percentage classification accuracy; it is defined as,

$$Acc(C) = \frac{\text{No. of correctly classified pixels}}{\text{Total no. of image pixels}} \times 100. \tag{11}$$

We show the simulation results for two specific examples: an instructive simulated example of satellite land cover data and a photographic colour image.

4.2. An instructive example

In this section we provide the proposed blind fusion results for the classification of two images shown in Figures 4(a) and 4(b). Figure 4(c) shows the actual true classification. The four classes are denoted by different grey levels. Image 1 (Figure 4(a)) is a synthetically degraded image. The true image was convolved with a Gaussian blur and additive white Gaussian noise with a blurred signal-to-noise ratio (BNSR) of 50 dB was added to the result. Image 2 (Figure 4(b)) is synthetically degraded as well with a multiplicative chi squared random noise process of degree 4. Image 2 can only differentiate two of the four classes shown in Figure 4(c).

The two images are passed through the proposed blind fusion method as shown in Figure 3. The user-specified parameter values used in the simulations are given in Table 1. The support of Image 1 for use in the NAS-RIF algorithm was estimated visually from that of Image 2. Plots of *Acc* vs. iteration and *Err* vs. iteration are shown in Figure 5. The algorithm is set to terminate when *Err* increases from one iteration to the next by a factor of at least ten. This terminates the NAS-RIF algorithm at iteration 6 which produces the best classification accuracy. The restoration and classification results at iteration 6 are shown in Figure 5.

*Calculation of $\sigma_{\tilde{w}}^2$ is given in Section 3.3.

Table 1. User-Specified Parameter Values used in the First Set of Simulations.

Algorithm	Parameter	Value
NAS-RIF	Dimensions of FIR filter u	5×5
NAS-RIF	Image support, D_{sup}	256×256
NAS-RIF	γ	1.0
MRF Classification	β_L	5
MRF Classification	*Threshold*	$10Err(C_0^{(k-1)}, C_L^{(k-1)})$

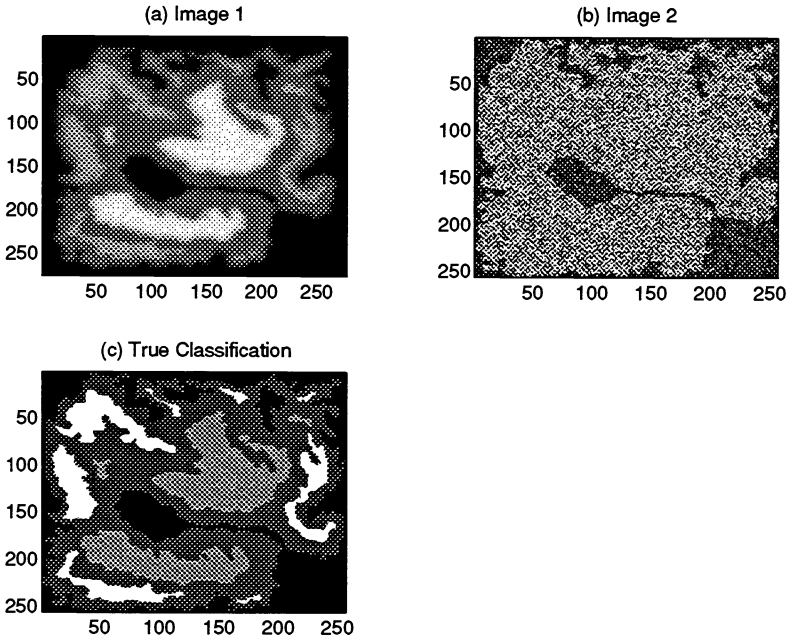

Figure 4. (a) Image 1: 276 x 276 image blurred with a Gaussian PSF and with a BSNR of 50 dB (The associated restored image is cropped to 256 x 256 so that it is registered with Image 2). (b) Image 2: 256 x 256 image degraded by multiplicative chi-squared noise process with eight degrees of freedom. (c) True Classification Results for 256 x 256 size image. Class 1 is denoted by black, Class 2 by dark grey, Class 3 by light grey and Class 4 by white.

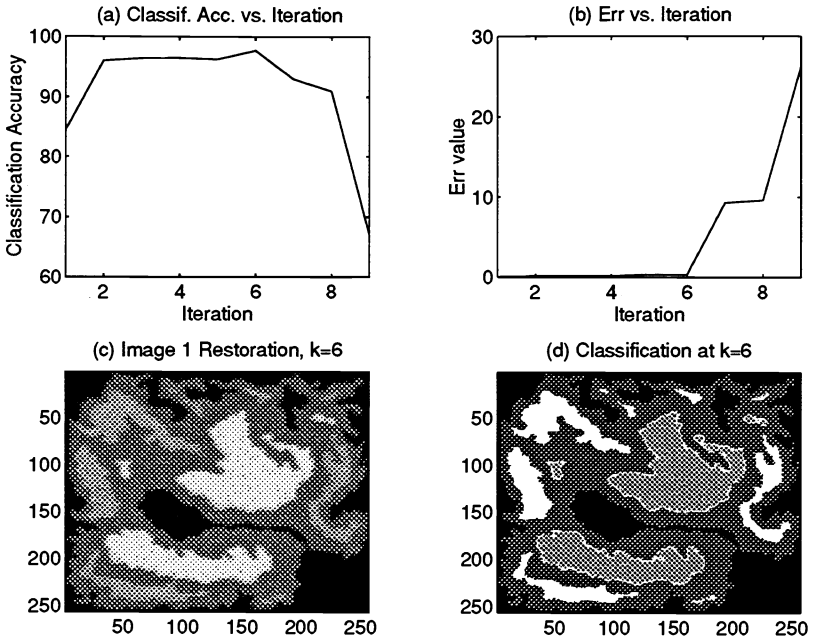

Figure 5. (a) Classification accuracy vs. iteration of the NAS-RIF algorithm. (b) The stopping criterion error as a function of iteration. (c) Restored Image 1 at the 6th iteration of the NAS-RIF algorithm. (d) Classification Result for the 6th iteration (corresponds to the result with the highest classification accuracy).

Table 2. User-Specified Parameter Values used in the Colour Image Simulations.

Algorithm	Parameter	Value
NAS-RIF	Dimensions of FIR filter u	5×5
NAS-RIF	Image support, D_{sup}	115×110
NAS-RIF	γ	1.0
MRF Classification	β_L	15
MRF Classification	*Threshold*	$2Err(C_0^{(k-1)}, C_L^{(k-1)})$

4.3. A colour image example

The method was also tested on the real colour image data of colourful crayons shown in Figures 6(a), 6(b) and 6(c). Image 1 is a blurred version (using a Gaussian PSF) of the original red band of the picture. Image 2 and 3 are low resolution versions of the green and blue bands, respectively. The true classification for this image was obtained by visual inspection and is shown in Figure 6(d). The grey-levels from light to dark represent the following classifications: yellow crayon, green crayon, purple crayon, red crayon and background, respectively.

Results of the blind fusion method are shown in Figure 7. The user-specified parameter values are shown in Table 2. The support information for the NAS-RIF algorithm was found as discussed for the previous example. Plots of *Acc* vs. iteration and *Err* vs. iteration are shown in Figure 7. The algorithm is set to terminate when *Err* increases from one iteration to the next by a factor of at least two. This terminates the NAS-RIF algorithm at iteration 14 which produces a classification accuracy of 93.3 %. The restoration and overall classification results are also given. It should be noted that the algorithm was not terminated exactly at the peak classification accuracy. The peak accuracy of 95.3 % was found at iteration 10. However, the termination point did produce a fairly reliable estimate.

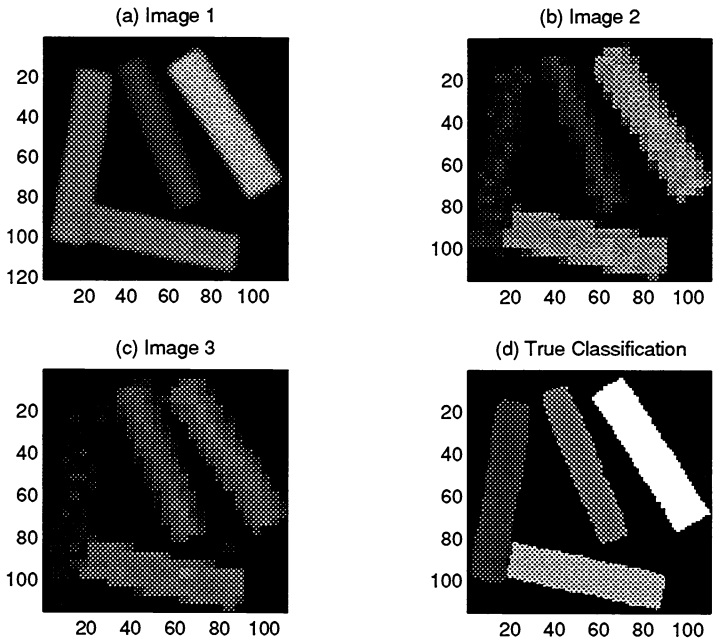

Figure 6. (a) Image 1: Blurred version of the red band of the original crayon image, (b) Image 2: Low resolution (by a factor of four) image of the green band, (c) Image 3: Low resolution (by a factor of four) image of the blue band, (d) True Classification Results. The classifications are distinguished according to grey-level. From brightest to darkest: yellow crayon, green crayon, purple crayon, red crayon and background.

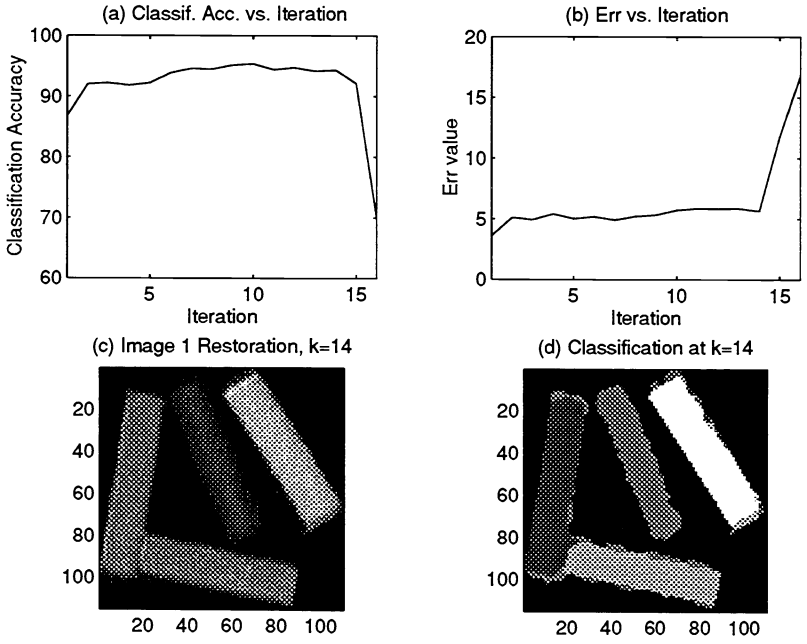

Figure 7. (a) Classification accuracy vs. iteration of the NAS-RIF algorithm. (b) The stopping criterion error as a function of iteration. (c) Restored Image 1 at the 14th iteration of the NAS-RIF algorithm. (d) Classification Result for the 14th iteration.

5. CONCLUSIONS

In this paper we present a novel approach to the robust fusion of blurred images. The proposed algorithm which involves the simultaneous deblurring and classification of multisensor imagery. The simulation results demonstrate the potential of the approach for practical blind image fusion.

ACKNOWLEDGEMENTS

This work was supported by the Canadian Department of National Defense under Contract 08SV.W7714-6-9990.

REFERENCES

1. M. A. Abidi and R. C. Gonzalez, *Data fusion in Robotics and Machine Intelligence*, Toronto: Academic Press, Inc., 1992.
2. D. Kundur and D. Hatzinakos, "Blind image deconvolution," *IEEE Signal Processing Magazine*, vol. 13(3), pp. 43–64, May 1996.
3. A. K. Jain, *Fundamentals of Image Processing*, Englewood Cliffs, New Jersey: Prentice-Hall Inc., 1989.
4. A. K. Katsaggelos, ed., *Digital Image Restoration*, chapter 1, New York: Springer-Verlag, 1991.
5. J. Biemond, R. L. Lagendijk and R. M. Mersereau, "Iterative methods for image deblurring," *Proc. IEEE*, vol. 78(5), pp. 856-883, May 1990.
6. B. Chandrasekaran and A. Goel, "From numbers to symbols to knowledge structures: artificial intelligence perspectives on the classification task," *IEEE Trans. on Systems, Man and Cybernetics*, vol. 18(3), pp. 415–424, May/June 1988.
7. T. Lee, J. A. Richards and P. H. Swain, "Probabilistic and evidential approaches for multisource data analysis," *IEEE Trans. Geosci. and Remote Sensing*, vol. 25(3), pp. 283- -293, May 1987.
8. J. A. Benediktsson, P. H. Swain and O. K. Ersoy, "Neural network approaches versus statistical methods in classification of multisource remote sensing data," *IEEE Trans. Gensci. Remote Sensing*, vol. 28(4), pp. 540–552, July 1990.
9. S. B. Serpico and F. Roli, "Classification of multisensor remote-sensing images by structured neural networks," *IEEE Trans. Gensci. Remote Sensing*, vol. 33(3), pp. 562– 577, May 1995.
10. K. S. Chen, D. H. Tsay, W. P. Huang, Y. C. Tzeng and D. T. Wang, "Terrain-cover classification by integration of SPOT and ERS-1 SAR images over Taiwan," *Proc. IGARSS-95*, vol. 3, pp. 1912–1914, 1995.
11. A. H. S. Solberg, T. Taxt and A. K. Jain, "A Markov random field model for classification of multisource satellite imagery," *IEEE Trans. Geosci. Remote Sensing*, vol. 34(1), pp. 100–113, Jan. 1996.
12. D. Kundur and D. Hatzinakos, "Blind image restoration via recursive filtering using deterministic constraints," IEEE Int. Conf. on Acoustics, Speech and Signal Processing, Atlanta, May 1996.
13. D. Kundur, *Blind Deconvolution of Still Images using Recursive Inverse Filtering*, M.A.Sc. Thesis, University of Toronto, 1995.